



# The Impact of Deorbiting Space Debris on Stratospheric Ozone

*Prepared for:*

Environmental Management Division  
Space and Missile Systems Center  
El Segundo, California

*Prepared by:*

TRW Space and Electronics Group

Peter D. Lohn, Ph.D.  
Eric Y. Wong, Ph.D.

*in coordination with:*

Mario J. Molina, Ph.D.  
Professor, Department of Earth and Planetary Sciences  
Massachusetts Institute of Technology

and

M. Richard Denison  
Denison Development Inc.

31 May 1994



# The Impact of Deorbiting Space Debris on Stratospheric Ozone

*Prepared for:*

Environmental Management Division  
Space and Missile Systems Center  
El Segundo, California

*Prepared by:*

TRW Space and Electronics Group

Peter D. Lohn, Ph.D.  
Eric Y. Wong, Ph.D.

*in coordination with:*

Mario J. Molina, Ph.D.  
Professor, Department of Earth and Planetary Sciences  
Massachusetts Institute of Technology

and

M. Richard Denison  
Denison Development Inc.

*Approved by:*



31 May 1994

# THE IMPACT OF DEORBITING SPACE DEBRIS ON STRATOSPHERIC OZONE

## CONTENTS

1. Introduction
2. Orbital Debris Population & Flux to the Stratosphere
3. Reentry Mechanics and Heating of Deorbiting Debris
4. Depletion of Stratospheric Ozone by Heterogeneous Mechanisms
5. Depletion of Stratospheric Ozone by Homogeneous Mechanisms
6. Summary and Conclusions

## 1. Introduction and Summary

The Environmental Management of the Space & Missile Systems Command has set out to evaluate the depletion of stratospheric ozone caused by Air Force activities in space. Potential destruction of ozone by launch vehicle exhaust is one item of concern (Ref. I. 1). The use of advanced propellants to minimize launch-induced ozone destruction is discussed in a companion report. The present report describes a quantitative assessment of another potential destroyer of stratospheric ozone: deorbiting space debris.

The results of the present study lead to the conclusion that deorbiting space debris has very little impact on stratospheric ozone. The task-by-task analysis leading to this conclusion is summarized as follows:

### Characterize the debris flux into the stratosphere.

Debris object density was characterized by size and altitude. Orbital decay was calculated and the results led to an estimate of the flux into the stratosphere as a function of object size. The results showed a preferential population of the stratosphere by smaller debris objects. The calculated stratospheric object density for one micrometer size particles is in reasonable agreement with measured values.

Calculate reentry trajectory and heating.

Several object sizes and materials were considered. In general, sub-millimeter size objects settle slowly through the stratosphere. Intermediate size objects (millimeter to decimeter) may melt/vaporize in or above the stratosphere. Larger objects (decimeters) may survive to the earth's surface. It is essential to account for the balance between convective heating and radiation heat loss to characterize the thermal response of the deorbiting debris. The trajectory/heating results provided initial conditions for assessment of ozone depletion by several mechanisms.

Evaluate ozone depletion by heterogeneous mechanisms.

Deorbiting debris provides several sources for deposition of small particles into the stratosphere. Two mechanisms, for example, are: direct orbital decay of small particles and stripping small particles from surfaces of larger space objects by aerodynamic drag forces generated during the deorbit/reentry process. The small particles provide active sites for heterogeneous reactions similar to those of the polar stratospheric cloud (PSC) particles. MIT performed experiments to measure the rate parameter for heterogeneous reactions in terms of the reaction probability. The measured data was used for the assessment of local and global effects on stratospheric ozone due to surface reactions. The impact on local ozone is evaluated based on a simple one-dimensional diffusion model for a single particle. Attention is focused on micrometer size particles because they provide the greatest total surface area. The resultant ozone depletion by heterogeneous mechanisms is estimated to be small:  $10^4$ - $10^6$  years to destroy one percent of the stratospheric ozone.

Evaluate ozone depletion by homogeneous mechanisms.

Deorbiting debris reentering the stratosphere at hypersonic speeds creates a high temperature region between the bow shock and the body. The temperature immediately behind the shock reaches temperatures as high as 20,000 degrees Kelvin. At such extreme temperature large amounts of nitric oxide will be produced according to the Zeldovich mechanism and ambient ozone is subsequently consumed through the nitric oxide catalytic cycle. An additional source of nitric oxide is generated as pyrolysis products from spacecraft paint or ablation materials (material bound nitrogen). The impact of these mechanisms on stratospheric ozone is estimated to be small: destruction of one stratospheric ozone molecule per one billion per day by the material-bound nitrogen mechanism and one part per ten billion per year by the thermal mechanism.

## 2. Orbital Debris Population & Flux into the Stratosphere

The debris environment is characterized by specifying object density as a function of altitude and size. A large body of experimental data has been used to evaluate the object density and it is an ongoing activity for several groups (e.g., U. S. Air Force, NASA) to continually upgrade the debris characteristics.

Data sources for the debris environment include:

- 1) U. S. Space Command radar data for objects of size greater than ten centimeters,
- 2) Impact data from objects retrieved from space (e.g., LDEF, Solar Max) for smaller objects. This requires estimation of debris characteristics from crater/impact features,
- 3) Additional radar data for objects in the one to ten centimeter range.
- 4) Estimates of booster/satellite breakup characteristics.

Present estimates (Reference 2.1) show the population at ~~7000~~ to 8000 objects of size 10 cm or larger, 35,000 to 150,000 objects in the 1- 10 cm range and 3-40 million under 1 cm. The altitude dependence of the object density is shown in Figure 2.1 (Reference 2.2) with the assumption of 35,000 objects of size greater than 1 cm. This population density can be scaled as the object density is updated. The flux of objects experienced by a spacecraft is the number density multiplied by a relative velocity (typically chosen as 10 km/s for LEO). The peak in object density at 800-1000 km is partly caused by booster breakup during launch of sun synchronous satellites while the peak at 1500 km is caused by breakup of NOAA satellite boosters as well as by USSR communication satellite activity.

Radar tracks 7000 objects.  $D > 10$  cm  
35000 objects with diameter  $> 1$  cm

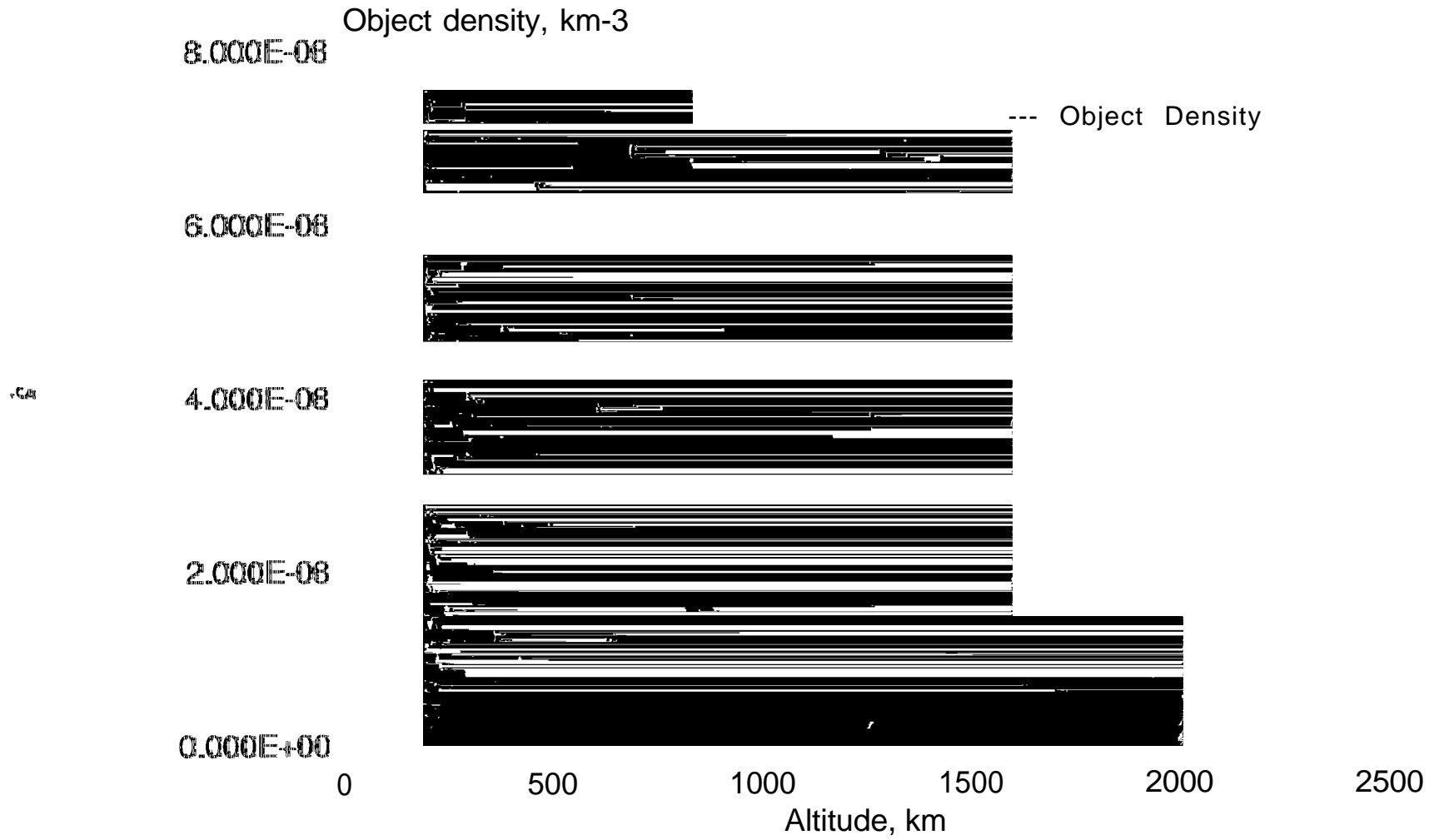


Figure 2.1. Orbital Debris Population

The orbital debris size distribution is a subject of continuing study. The size distribution used for this study is shown in Figure 2.2 and is taken from Reference 2.3. The ordinate of Figure 2.2 gives the number of particles of size greater than diameter  $d$ . The distribution is plotted from an analytical expression that gives approximately 7000 objects of size 10 cm or greater. While the figure shows the population increasing several orders of magnitude for the smaller size objects the object density may be overpredicted for object size less than 0.001 cm or 0.01 cm (Reference 2.4).

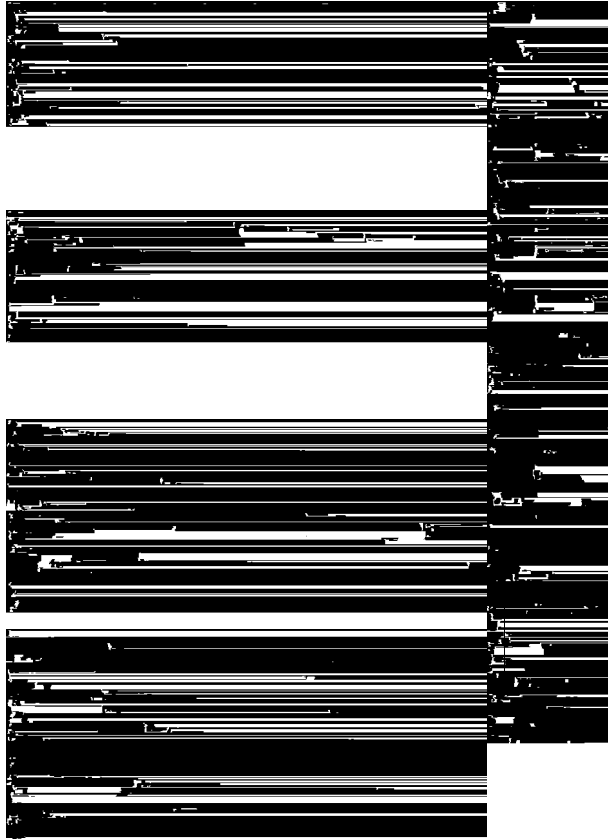
The debris population is increasing as a result of newly launched objects, explosions, collisions, and breakup of boosters and spacecraft. An estimate of the yearly growth of the debris population is given in Reference 2.3:

- o five percent for intact objects
- o two percent for fragments (increasing to four percent after the year 2010).

The debris object density and the subsequent flux into the stratosphere should be increased at these rates for later years.

## FLUX INTO THE STRATOSPHERE

The process of orbital decay involves all the forces experienced by an object in space. The final decay process (altitudes below several hundred kilometers) is dominated by aerodynamic drag caused by the earth's atmosphere. A complete characterization of the decay process must include a balance of production terms (caused by new launches and



6  
6  
6



fragmentation) with the orbital decay process. Such a complete model is beyond the scope of this project and thus we take the available estimates of object population and size/mass distribution and subject these objects to the orbital decay process. We have used average material density estimates from Reference 2.3 for our decay analysis:

- o 4.0 g/cm<sup>3</sup> for diameter less than or equal to 0.62 cm,
- o  $2.8 d^{0.74} \text{ g/cm}^3$  for diameter greater than 0.62 cm (d in cm).

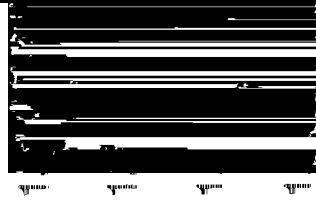
A spherical geometry is assumed. The density of larger objects is reduced to account for irregular shapes such as hollow structures.

The deorbit time (time for the object to reach 50 km as a result of atmospheric drag) was calculated for objects initially at altitudes from 200 to 1200 km and for sizes from 0.0001 to 100 cm. The calculation was made assuming a solar radio flux index of 1 SO (which is about an average value, which results in about an average atmospheric density, which results in an average estimate of drag, and which predicts an average estimate of orbital decay time) and is based on the present 1994 object density (and hence should have a growth factor applied for later years). The calculations are conservative (smaller decay time) in that circular orbits were assumed.

The resulting flux into the stratosphere is given in Figure 2.3 as a function of object size. The flux is constructed by combining deorbit times from altitudes from 200 km to 1200 km and for object sizes from 1  $\mu\text{m}$  to 100 cm. While an object is in orbit the decay rate is directly proportional to the weight to drag ratio of the object: large objects take longer to deorbit than do smaller objects. When the object enters the stratosphere and begins the

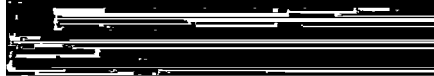
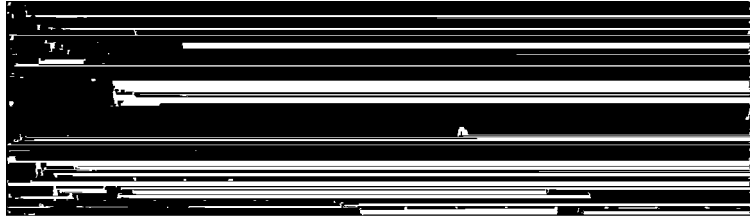


1.000E+06



1.08 W+01

1.000E+00



10-20



10

reentry process aerodynamic drag decelerates smaller objects more than the larger objects.

The resultant effect is that the population of debris in the stratosphere will be biased toward the smaller objects. The population of smaller objects in the stratosphere will be further increased by several mechanisms:

- object breakup as a result of the reentry process;
- stripping of particulates from the surface of larger objects by aerodynamic drag during deorbit-approximately  $10^6$ - $10^7$  micrometer-sized particles per square foot are attached to an orbiting object with, perhaps, thousands of square feet of area per spacecraft (Ref. 2.5);
- potential solidification of small droplets (produced from melting/ablating during reentry);
- particulates in materials such as paints that are released when binder materials melt during reentry heating (Ref. 2.6).

### 3. Reentry Mechanics and Heating of Deorbiting Debris

Understanding the reentry of the orbital debris objects requires consideration of several effects:

- 1) deorbit conditions (at about 120 km);
- 2) reentry trajectory;
- 3) aerodynamic heating;
- 4) heating of the debris object and possible melting or vaporization.

The evaluation is further complicated by the myriad of debris sizes, shapes, and materials.

Reentry trajectories are calculated using a three degree-of-freedom trajectory analysis. The initial conditions for the analysis were chosen as the orbital velocity at 120 km, 7825 m/s. A range of initial flight path angles were considered. A key component to the trajectory determination is assessment of the drag coefficient. We have used drag coefficients applicable to spherical (or near-spherical) objects as well as tumbling drag coefficients for cylindrical-like objects (we should be very clear here and point out that we must treat representative rather than specific object shapes). The actual drag coefficient is “bridged” between the free-molecule value and the continuum value (transitional flow regime). Bridging is necessary to make reentry analyses tractable. We have based our bridging functions on evaluation of data and analysis for various blunt bodies (References 3.1 & 3.2).

Sample drag coefficients for continuum and free-molecule flow are:

Object Type	Continuum Drag Coefficient, $C_c$	Free-Molecule Drag Coefficient, $C_{FMB}$
Sphere	0.9	2.1
Tumbling cylinder	1.05	2.4

The bridging function **used** for drag is

$$\phi = \frac{Kn}{Kn + 0.3}.$$

where the Knudsen number is the free stream, ambient, mean free path divided by the appropriate reference length ( *e.g.*, the sphere diameter).

The drag coefficient is thus constructed by

$$C_D = C_c + \phi ( C_c - C_{FMB} ).$$

The drag entered into the equations of motion is thus

$$\frac{1}{2} \rho V^2 \times Area \times C,,$$

where  $\rho$  is the ambient density,

V is the vehicle velocity,

and Area refers to the object reference area.

The aerodynamic heating is also characterized by a bridging function (except for small Knudsen numbers e.g.,  $Kn \leq 0.05$ ). The bridging function for stagnation point heat transfer is:

$$\phi = Kn / (Kn + 0.1).$$

The continuum value for stagnation point heat transfer is (Refs. 3.3, 3.4, 3.5, 3.6)

where  $\rho$  is ambient density in kg/m<sup>3</sup>.

V is debris velocity in m/s,

and R is the effective radius of the debris object, in meters.

Heating of the reentering debris object is a balance of aerodynamic heating and heat loss by radiation. The radiant heat loss by the object was assumed to be to a 300K sink (earth) over one half of the object surface area and to a 0K sink (space) over the remaining half of the objects area. A surface emissivity of 0.8 is assumed:

$$W/m^2$$

The stagnation point heat transfer is experienced only near the objects stagnation point. The stagnation value is averaged over the object surface in order to account for the tumbling motion of the vehicle and for the localized high stagnation heating. Guidelines for this averaging are given by Cropp (Reference 3.2) for several shapes. As an example, for a sphere the freestream heat flux is multiplied by a factor of 0.275 while the continuum value is multiplied by 0.25.

Trajectory/heating assessments were made for a collection of object sizes, shapes, and materials. The temperature of the reentering debris object was calculated by evaluation of the net heating of the object and the thermal mass (capacity) of the object. A result of particular interest was the altitude at which the melting temperature of the object was reached: at this point the debris object is expected to breakup into droplets and/or vaporize and the reentry process will cease. A second result of interest is the altitude where the object temperature reaches 450 K. At approximately 450K paints, epoxies, resins, and other composite materials will decompose with the possibility of formation of NO, and the subsequent depletion of ozone.

Physical properties for selected materials are given in the following table:

material	density, kg/m <sup>3</sup>	specific heat, cal/gm/K	melting point, K	thermal conductivity, W/m/K
Aluminum	2700	.22	870	240
Beryllium	1850	.44	1560	220
Stainless Steel	7800	.10	1500	45
Titanium	4500	.12	1930	20
Magnesium	1740	.24	870	160

The deorbiting/heating process is a balance of the drag and mass which determines the velocity/altitude state vector of the deorbiting event. The velocity/mass and object geometry determines the heating rate. The thermal capacity of the object along with the heating history determines the object temperature. And, finally, the object melting point is an important factor which determines whether or not the object deorbits, melts or evaporates, or, in the case of a complex object such as a spacecraft breaks up into smaller objects.

A number of calculations were made for objects with the recommended material density,

- 4.0 g/cm<sup>3</sup> for diameter less than or equal to 0.62 cm,
- 2.8 d<sup>0.74</sup> g/cm<sup>3</sup> for diameter greater than 0.62 cm (d in cm).

and with the heat capacity of aluminum. These results are shown in Figures 3.1-3.12. The net heat flux to the object (convective-radiative) is plotted along with the material bulk temperature. As the objects encounter the rapidly increasing density with decreasing altitude they began to experience drag (which slows the object) and heating (which increases the objects temperature. The very small particles decelerate rapidly, do not heat significantly, and drift into the stratosphere at a very low velocity (the long time for a very small particle to drift through the stratosphere is shown in Figure 3.13). The very large particles may survive because the thermal mass is sufficient to avoid reaching the melting temperature (and possibly avoid breakups caused by the state of stress set up by the aerodynamic loads- exacerbated by high temperature) ~~and~~ because the body is sufficiently blunt to avoid high stagnation point heating (the  $R_{nose}^{-0.5}$  effect: a blunt nose reduces stagnation point heating during hypersonic reentry). The intermediate size particles however enter the high density atmosphere with high velocity. They experience high stagnation heating and are heated to relatively high temperature. The intermediate size objects described in Figures 3.3-3.8 reach the melting point of aluminum above the stratosphere. The results obtained the present analysis are consistent with results reported in Reference 3.7 (lower heat flux for smaller objects-lower ballistic coefficient) and Reference 3.8 (reentry survivability of large spherical objects).

Sphere Diameter= 0.001 cm  
@ 122000. m:  $v_t = 7673$  km/s  
and  $\gamma = 0.0$

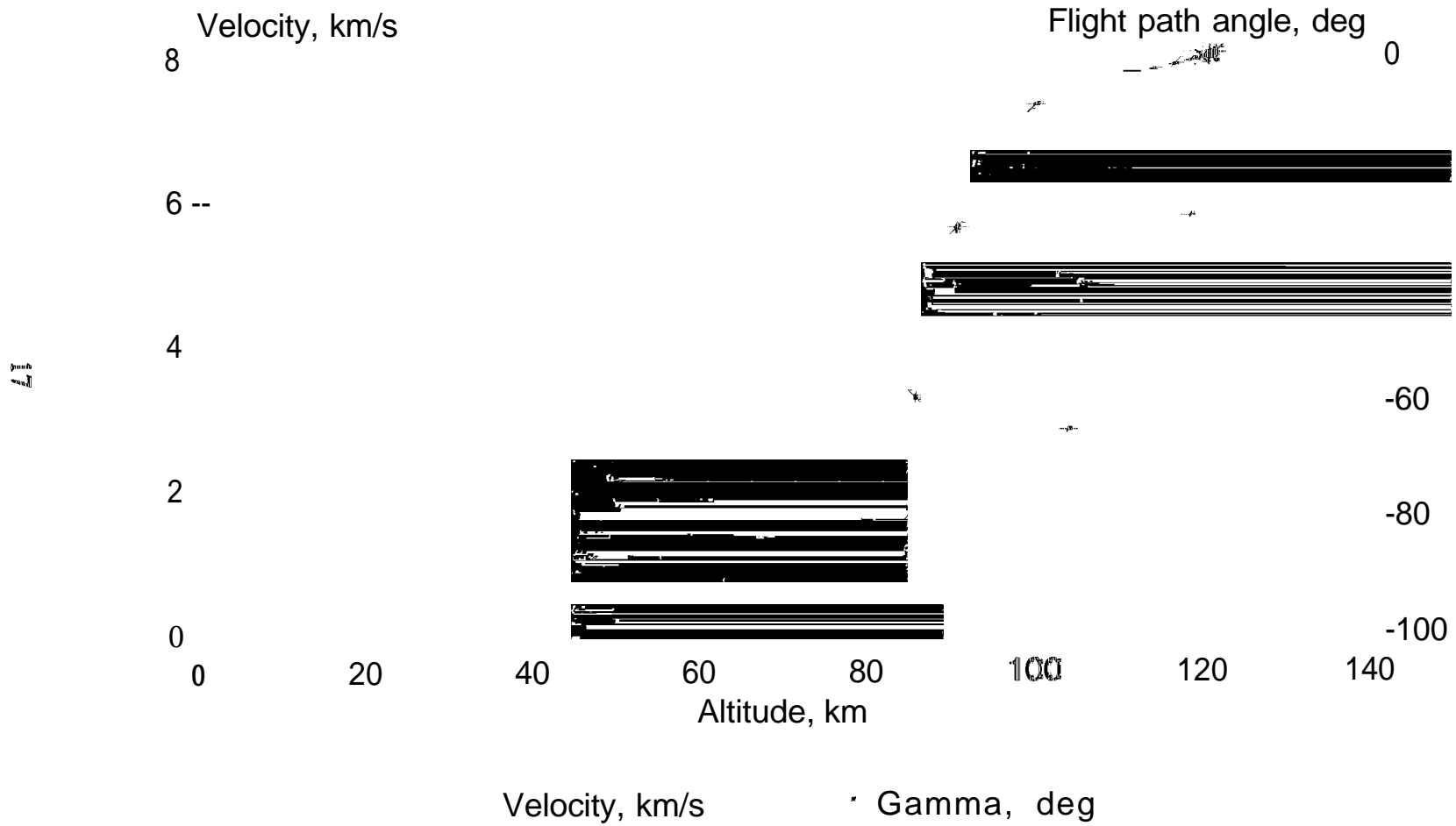
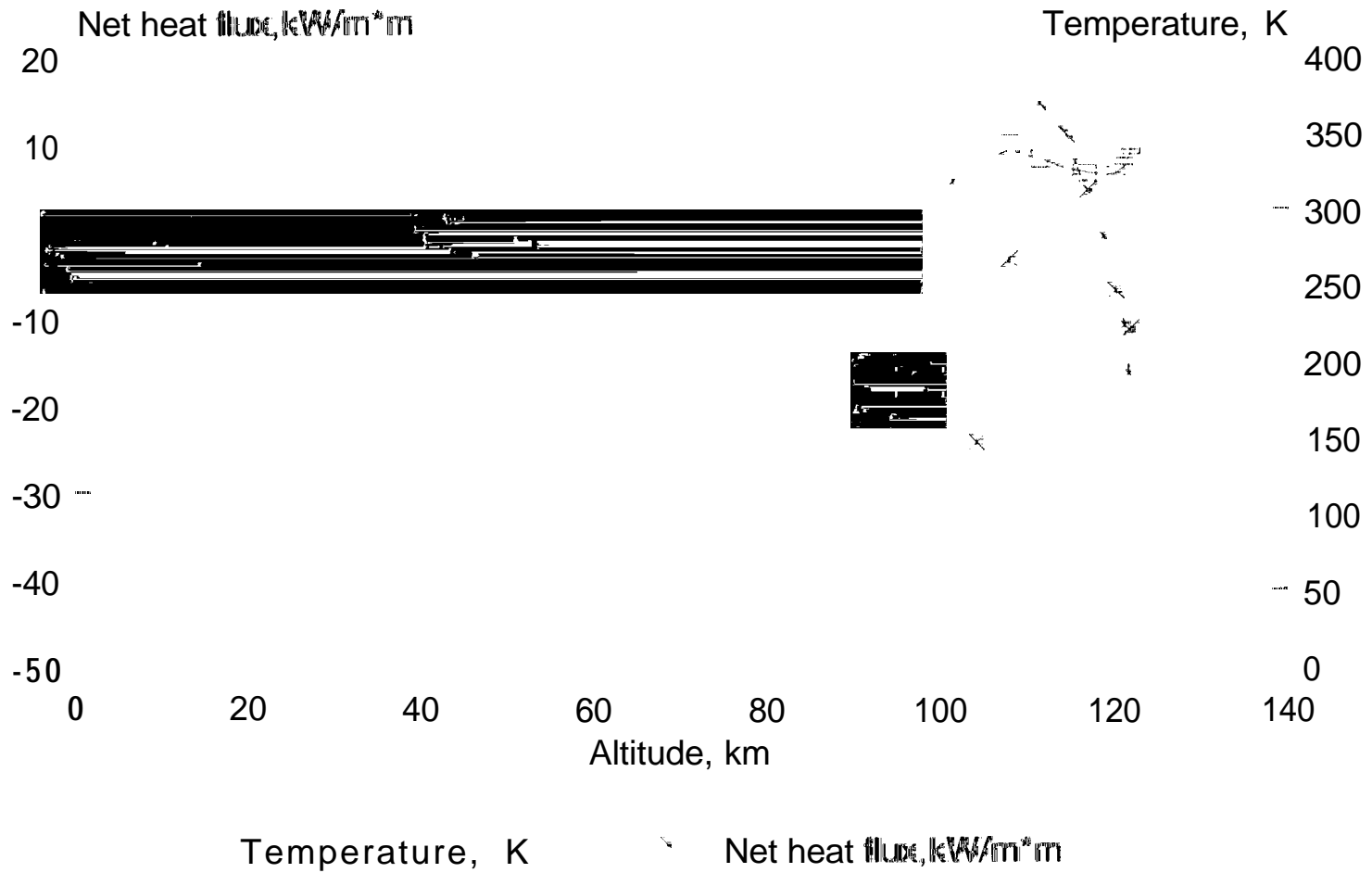


**Figure 3.1.**

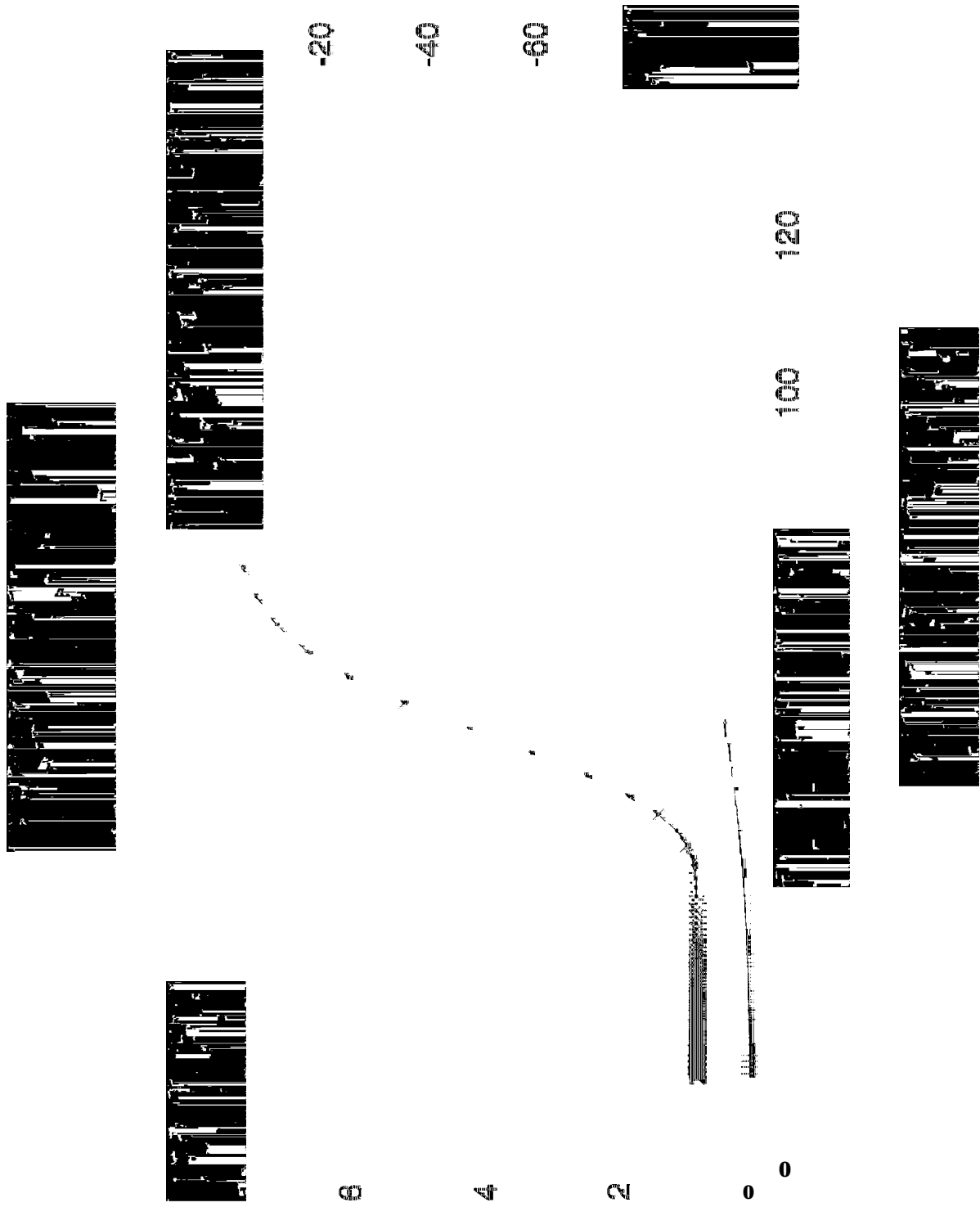
Aluminum: recommended density

Sphere Diameter= 0.001 cm  
 @ 122000. m:  $v_t=7673$  km/s  
 and gamma= 0.0



Aluminum: recommended density

Figure 3.2.



Aluminum: recommended density

Sphere Diameter= 0.10 cm  
 @ 122000. m:  $v_t=7673$ . km/s  
 and gamma= 0.0

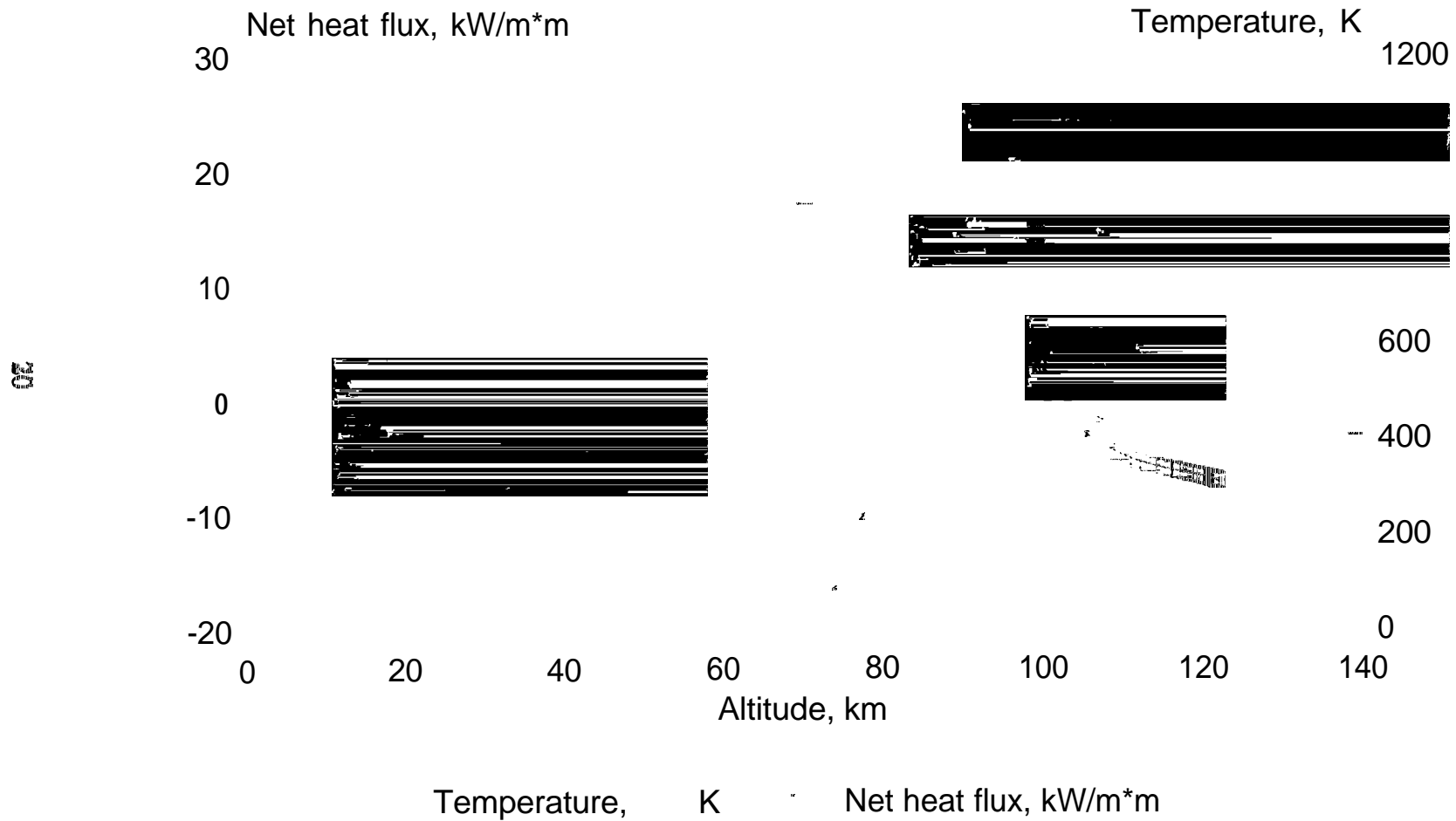
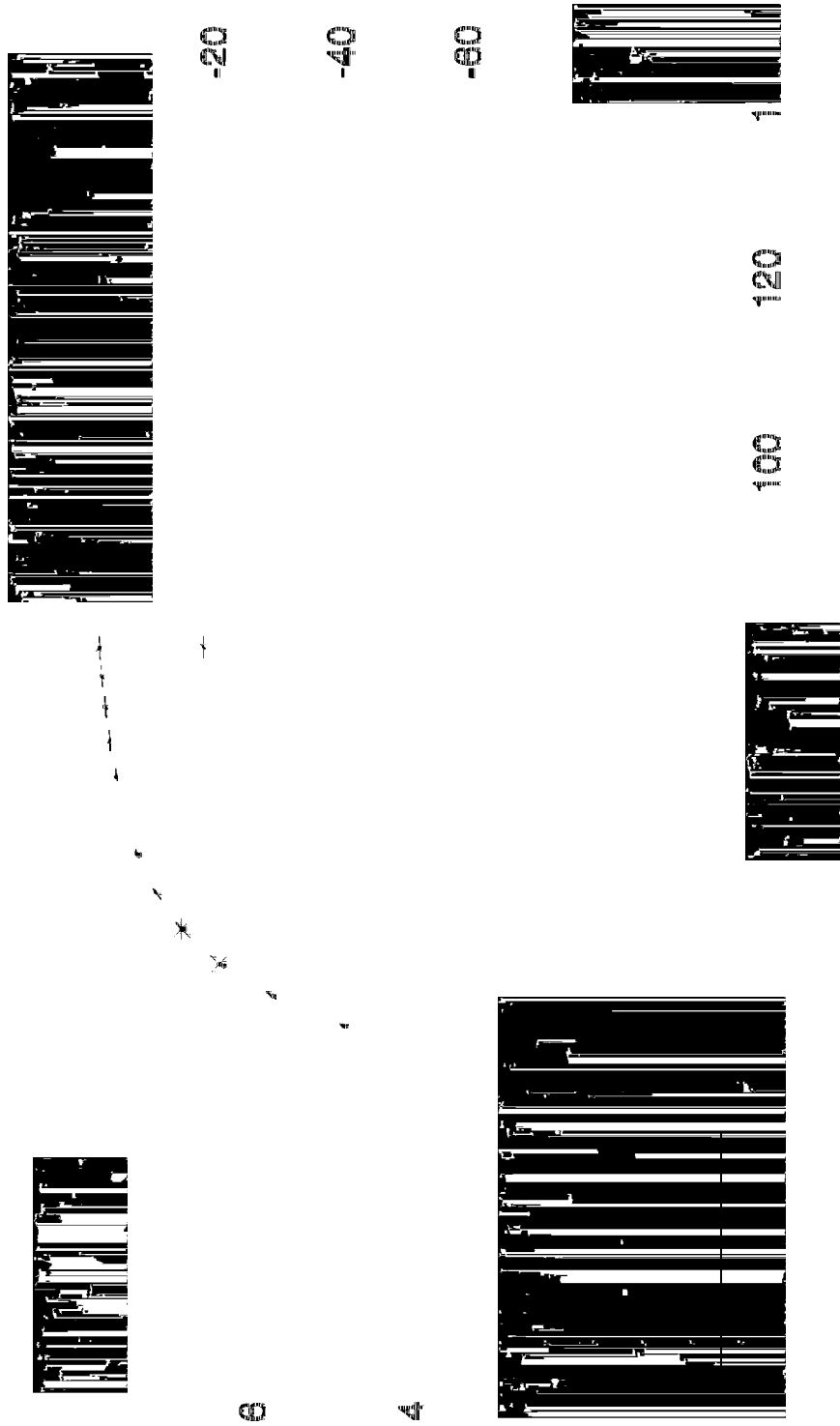


Figure-3.4

Aluminum: recommended density

Soft  
Sf  
®



Aluminum: recommended density

0591

049

00

00

Aluminum

























































































































